ELSEVIER

Journal of Nuclear Materials 295 (2001) 149–156

journal of nuclear materials

www.elsevier.nl/locate/jnucmat

Compatibility tests of steels in flowing liquid lead–bismuth

F. Barbier [a], G. Benamati [b,*], C. Fazio [b], A. Rusanov [c]

[a] *CEA-CEREM/SCECF, CE Saclay, Gif-sur-Yvette cedex 91191, France*
[b] *ENEA, Divisione Fusione, CR Brasimone, 40032 Camugnano, Bologna, Italy*
[c] *IPPE, Bondarenko Square 1, Obninsk, Kaluga Region, 249020, Russia*

Received 18 December 2000; accepted 29 March 2001

Abstract

The behaviour of steels exposed to flowing Pb–55Bi was evaluated. The materials tested are the two austenitic steels AISI 316L and 1.4970, and the six martensitic steels Optifer IVc, T91, Batman 27, Batman 28, EP823 and EM10 which were exposed to flowing Pb–55Bi for 1000, 2000 and 3000 h and at two temperatures (573 and 743 K). The corrosion tests were conducted in the non-isothermal loop of IPPE-Obninsk under a controlled oxygen level (10^{-6} wt%). The compatibility study showed that at a lower temperature, a very thin oxide layer (<1 μm) was formed on the steels. At higher temperature, austenitic steels also exhibited a thin oxide layer sufficient to prevent their dissolution in the melt. A thicker oxide, which grew according to a parabolic law, was observed on the surface of the martensitic steels. The oxidation resistance behaviour of the martensitic steels was correlated with their alloying elements. © 2001 Published by Elsevier Science B.V.

1. Introduction

Accelerator-driven systems (ADS) for energy production and destruction of actinides by transmutation are promising concepts [1]. Such systems reply on the production of spallation neutrons that occur when high-energy protons from accelerators slam into target materials. Then, the neutron source is arranged in a subcritical blanket for transmutation. To avoid parasitic neutron losses in such a design, the use of a low neutron-absorbing material is preferred. Liquid lead–bismuth eutectic (Pb–55 at.% Bi) is a potential candidate for both the target material and coolant. The use of Pb–Bi liquid metal targets as compared to liquid Pb offers the advantage of a lower melting point (398 vs. 600 K). Further, the liquid PbBi has also a low vapour pressure, good neutron yield, fast heat removal, and no structural damage due to irradiation.

Austenitic steels are candidate materials for the vessel and in-vessel components of an ADS-DEMO reactor and the 9–12 Cr martensitic steels are candidate materials both for the core and for the spallation target. In any liquid metal application, the compatibility of the container material with the liquid metal must be considered since it is recognised that liquid metals can have corrosive properties. From the literature, it is known that severe corrosion occurs in the presence of liquid lead alloys, especially at high temperature [2]. For example, nickel is much more soluble than iron and chromium in Pb alloys so that corrosion of austenitic steel has to be considered seriously. The selection of the structural material exposed to Pb–Bi is thus a complex issue and compatibility studies are required.

The lead–bismuth technology was initially developed in Russian submarines and, in order to take advantage of this experience, ENEA (Italy) and CEA (France) have started collaborative programmes with the Institute of Physics and Power Engineering (IPPE) at Obninsk, Russia. Both ENEA and CEA proposed several steels to be tested in controlled conditions in the CU-1M liquid metal loop at IPPE. The behaviour of different austenitic and martensitic steels was compared to that of the Russian ferritic–martensitic steel when exposed to

* Corresponding author. Tel.: +39-0534 801 179; fax: +39-0534 801 225.
E-mail address: benamati@brasimone.enea.it (G. Benamati).

0022-3115/01/$ - see front matter © 2001 Published by Elsevier Science B.V.
PII: S0022-3115(01)00570-0

flowing Pb–Bi at 573 and 743 K. In addition, the oxidation behaviour of the martensitic steels observed at 743 K was analysed and an attempt was made to correlate the corrosion rate to the steel grade and the quantity of alloying elements.

2. Experimental

The tests were performed in the experimental facility of IPPE. The CU-1M loop (volume ≈60 l) – comprising a central heat exchanger, a hot leg, a cold leg and a tank for filling and draining – was used. The hottest parts were made of 20Cr–14Ni–2Si austenitic steel and the low-temperature parts ($T < 693$ K) were of 18Cr–10Ni–1Ti steel. The heat exchanger was made of 13Cr–2Mo–2Si martensitic steel. A centrifugal pump moved the alloy through the circuit with a velocity measured by an electromagnetic flowmeter. The oxygen content in Pb–Bi was maintained constant with time. A gas system (He–20% H_2) and a system allowing PbO dissolution were connected to the loop for oxygen removal and replenishment, respectively. The oxygen concentration was measured by means of two electrochemical sensors placed in the hot section.

The operating temperature (T) was 743 K in the hottest section and 573 K in the cold-test section, the coldest point in the loop being 523–533 K. The flow velocity was (1.9 ± 0.1) m/s and the oxygen concentration in Pb–Bi (c_{O_2}) was maintained at $(1–2) \times 10^{-6}$ wt%.

The composition of the Pb–Bi alloy was (wt%): 44.42Pb–55.77Bi–3.3×10^{-4}Fe–2.8×10^{-3}Ni–$<10^{-3}$Cr. Six martensitic steels (Optifer IVc, EM10, T91, Batman 27, Batman 28 and Russian steel EP823) and two austenitic steels (1.4970, AISI 316L) were tested, the chemical compositions of which are indicated in Table 1. The corrosion specimens, cylinder shaped, were 110 mm high with a diameter of 8 mm; the ends of the cylinder were machined with a lower diameter in order to fit the specimens in the test sections. The specimens were fixed in the hot- and cold-test sections of the loop with the duration of exposure ranging from 1000 to 3000 h.

At the end of the tests, the specimens were taken out of the loop and cleaned for visual examination. Finally, pieces were cut and polished for cross-section examination by optical and scanning electron microscopy (SEM). Chemical analyses were obtained by SEM via energy dispersive X-ray (EDS – the quantitative evaluation of the elements was made by applying the ZAF-correction procedure) and by electron microprobe analysis. In addition, X-ray diffraction (XRD) was used for compound characterisation.

3. Results

3.1. Martensitic steels

3.1.1. Batman 27 and 28 steels

At low temperature (573 K), the visual inspection showed that the surface of the three samples tested for 1000, 2000 and 3000 h was coloured black. The metallurgical analysis performed on the transversal section indicated that a thin scale, not uniformly distributed, was formed on the surface of the 2000 and 3000 h tested samples. The XRD pattern, recorded on the surface of the samples, showed diffraction peaks corresponding to the (3 1 1), (4 0 0), (5 1 1) and (4 4 0) diffraction planes of Me_3O_4 (Me = Fe, Cr)-type oxide for the highest exposure time (3000 h).

Higher testing temperature (743 K) produced an increase in the oxide layer thickness. A distinct scale uniformly distributed on the surface could be detected by analysing the cross-sections of the three samples exposed for 1000, 2000 and 3000 h. The morphology of the corrosion products could be compared to a multiple-layer structure with the outer layer appearing less compact than the inner one. In the SEM micrographs, the corrosion product has a two-layer structure after 1000 h (Fig. 1(a)) whereas after 2000 and 3000 h, three layers

Table 1
Chemical compositions of the steels (wt%)

	Cr	Ni	Mo	Mn	V	Nb	W	Ti	Si	C
Austenitic steel										
1.4970	15.4	14	1.8	2.4	–	–	–	0.4	0.5	0.12
AISI 316L	17.3	12.1	2.31	1.8	–	–	–	–	0.35	0.02
Martensitic steel										
Optifer IVc	9.1	–	–	0.52	0.22	–	1.4	–	–	0.12
EM10	9.0	0.1	1.0	0.5	–	–	–	–	0.3	0.1
T91	8.26	0.13	0.95	0.38	0.20	0.075	–	–	0.43	0.105
Batman 28	8.94	0.05	0.01	3.51	0.24	0.01	1.51	0.01	0.32	0.09
Batman 27	9.0	0.07	0.01	3.1	0.21	0.01	1.45	0.20	0.49	0.1
EP823	12	0.89	0.7	0.67	0.43	0.4	1.2	–	1.8	0.14

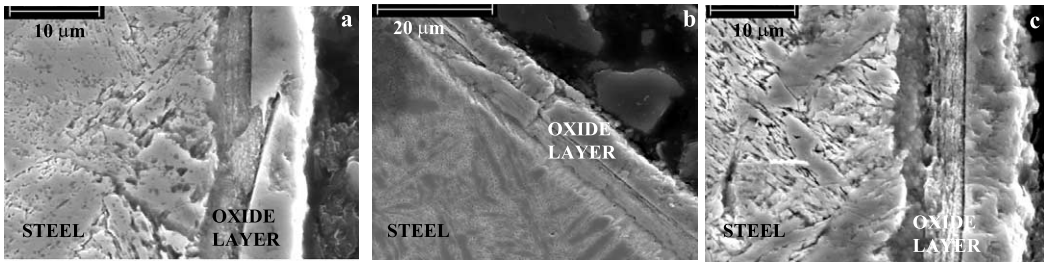

Fig. 1. SEM micrographs of the Batman 28 steel transversal sections tested at 743 K for: (a) 1000 h; (b) 2000 h; (c) 3000 h.

were evident (Figs. 1(b) and (c)). The widths of the corrosion layers were measured both on the Batman 27 and Batman 28 steels. The average thickness measured on Batman 27 (Batman 28) was about 10 (12) μm, 13 (15) μm and 15 (17) μm after 1000, 2000 and 3000 h of exposure, respectively. With regard to the composition of the corrosion products, the elemental analysis performed on Batman 28 samples with the EDS detector indicated that the outmost layer of the 1000 h specimen is composed mainly of O, Fe and Mn. The internal layer adjacent to the steel surface contains the main elements of the steel and oxygen. The concentration profile diagram recorded on the 2000 h tested sample is shown in Fig. 2. The composition of the outmost layer is comparable to that of the 1000 h tested sample; the intermediate layer is composed of O, Cr and Fe, where the Cr content is in between 14–15 wt%. In the third layer, the Cr content is comparable to that of the bulk material and the O content decreases through the layer towards the steel. The 3000 h exposed sample exhibited a corrosion layer, the composition of which is comparable to that of the 2000 h tested sample. The other alloying elements of the steel, Mn and W, were detected in the corrosion layers of the three samples. The content of Mn was about 2 wt% in the outer layer, and about 2–3 wt% in the inner for each exposure time. W was not detected in the outer layer of the three samples and the content of W in the inner layers was about 2 wt%. The XRD patterns recorded on the surface of the tested steel specimen showed, for the three exposure times, the peaks of the Me_3O_4 oxide, with Me = Fe, Mn and Cr.

3.1.2. EM 10 steel

As previously, the surface of the three EM10 specimens tested at 573 K for 1000, 2000 and 3000 h was coloured black. Analysing the transversal section, on the surface of the 2000 h and 3000 h tested samples, a thin oxide scale was observed not uniformly distributed with similar features as reported for the Batman steels.

At 743 K, for the three exposure times, corrosion products were observed on the surface of the samples. By electrochemical etching with oxalic acid (10%), it was possible to reveal a double-layer structure of the corrosion products for the three exposure times. The morphologies of the layers were similar to those of the Batman steels, even if in some places of the EM10 steel, the presence of Pb–55Bi was observed between the two layers. The infiltration and/or embedding of the liquid alloy were more evident with higher testing times. The thickness of the corrosion products evaluated in the zones without Pb–55Bi was observed to be 15 μm after 1000 h exposure, 17 μm after 2000 h exposure and 22 μm after 3000 h exposure.

As far as the distribution of Fe and Cr in the corrosion products is concerned, it could be observed that it was comparable to that of the Batman steels. With

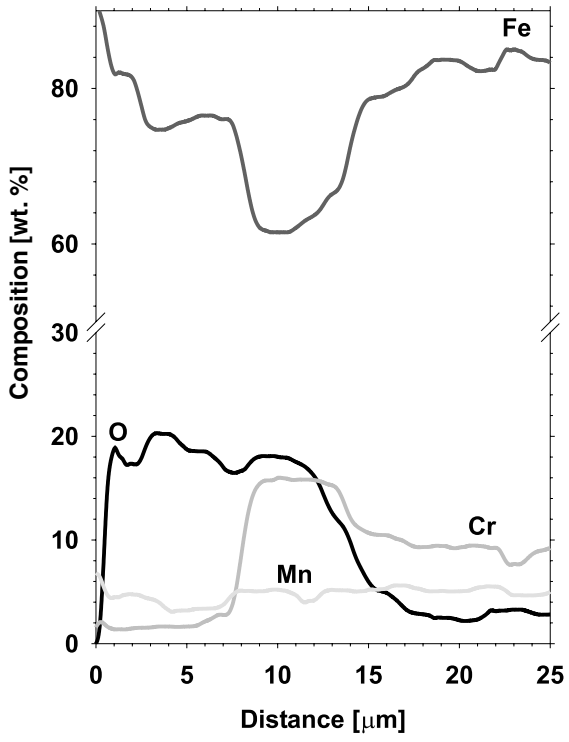

Fig. 2. Concentration profile recorded on the Batman 28 sample tested at 743 K for 2000 h.

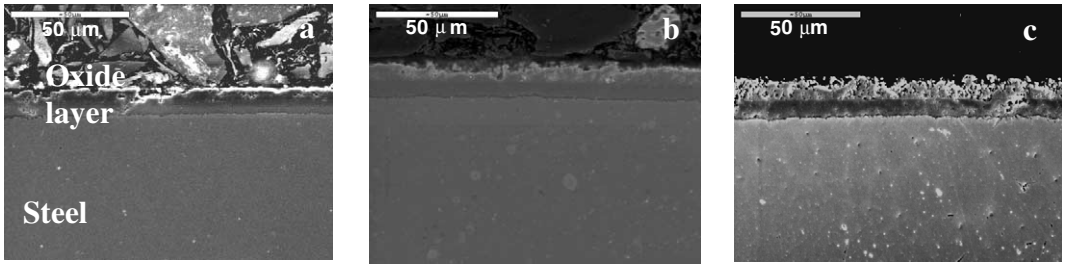

Fig. 3. SEM micrographs of the T91 steel tested at 743 K for: (a) 1000 h; (b) 2000 h; (c) 3000 h.

regard to the alloying elements of the EM 10 steel, Mo was not detected in the outmost layer of the corrosion products, and the content of Mo in the inner layer was about 2 wt% for the three testing times.

3.1.3. T91 steel

At 573 K, the black-coloured surface of specimens tested from 1000 to 3000 h exhibited a non-uniform oxide scale. The thickness was very thin and measurements were not possible, as the oxide was only present at some points.

At higher temperature (743 K), the behaviour was quite different. A regular oxide layer with thickness increasing with time was observed (11, 14 and 16 μm after 1000, 2000 and 3000 h of exposure, respectively). The layer on the steel surface is composed of two zones, porous in the outer and compact in the inner part (Fig. 3). A Cr enrichment is observed in the internal part as shown by the concentration profiles: maxima in Cr concentrations are accompanied by minima in Fe concentrations (Fig. 4). The presence of magnetite scale is confirmed by its XRD pattern, which exhibited the peaks corresponding to the diffraction planes (3 1 1), (4 0 0), (5 1 1) and (4 4 0). The analyses indicated compositions Fe_3O_4 in the external part and $(Fe,Cr)_3O_4$ in the internal part.

3.1.4. Optifer IVc steel

Whatever the temperature, the behaviour of Optifer IVc steel is very similar to that of T91, with the exception that the thickness of the oxide layer is much larger at 743 K (Fig. 5). It varies from 16 μm for an exposure time of 1000 h to 22 μm after 3000 h. The distribution of the elements through the oxide scales corresponds to Fe_3O_4 in the external part which is depleted in Cr and $(Fe,Cr)_3O_4$ in the internal part [4]. For this steel, the morphology of the porous outer layer exhibited irregularities in some places, which is possibly indicative of scale removal.

3.1.5. EP823 steel

At low temperature, the oxide layer formed on the steel surface was non-uniform and extremely thin. At 743 K, a regular oxide layer was observed (Fig. 6). It was also composed of two zones as in the case of EM10, T91and Optifer IVc steels. However, its thickness was reduced, varying from 6 μm for an exposure time of 1000 h to 10 μm after 3000 h. The internal part of the oxide layer is enriched with chromium and also with silicon, while the external part composed of Fe_3O_4 is practically free of alloying elements [4].

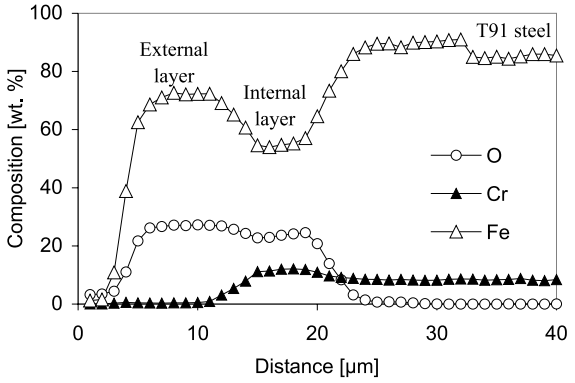

Fig. 4. Concentration profiles obtained on T91 steel tested at 743 K for 3000 h.

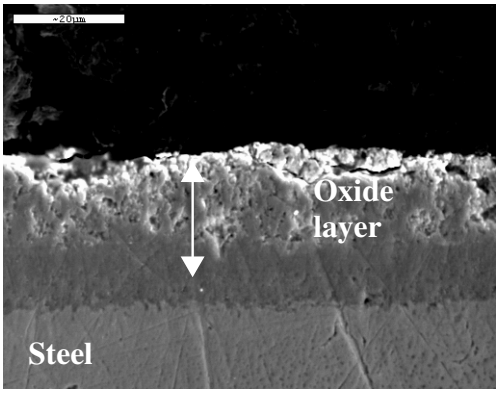

Fig. 5. SEM micrograph of the Optifer steel tested at 743 K for 3000 h.

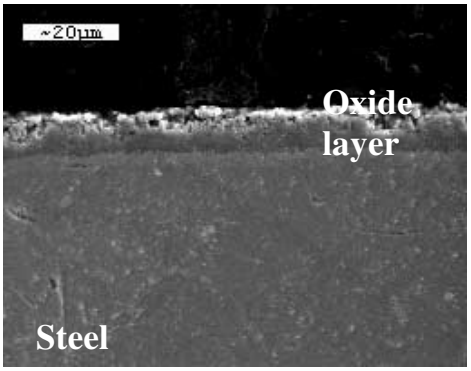

Fig. 6. SEM micrograph of the EP823 steel tested at 743 K for 3000 h.

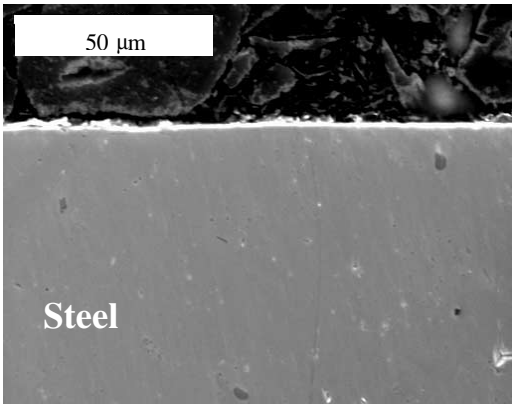

Fig. 7. SEM micrograph of the 1.4970 steel tested at 743 K for 3000 h.

3.2. Austenitic steels

3.2.1. AISI 316L steel

By analysing the cross-section of the austenitic steel tested at both temperatures, it seemed that it did not undergo extended oxidation nor dissolution of the steel elements during the contact with Pb–Bi in the hereinreported testing conditions. For the specimens tested in the most severe conditions (743 K for 3000 h), an austenitic grain structure was revealed after electrochemical etching with the oxalic acid solution (10%) and no ferritic layer characterised by preferential Ni depletion was observed. The absence of such a layer (a typical feature of austenitic steels exhibiting dissolution in liquid lead alloys [3]) indicated that no liquid metal corrosion took place during exposure to Pb–Bi, confirming the presence of a thin protective oxide layer on the surface, even if it was not detected by SEM.

3.2.2. 1.4970 steel

As for AISI 316L steel, no sign of liquid metal corrosion damage characterised by Ni dissolution was observed at 573 and 743 K (Fig. 7). The concentration profiles shown in Fig. 8 indicate no change in the distribution of steel elements, and thus, no dissolution occurred at the interface. In fact, a very thin protective oxide layer (not detected by SEM) is formed on the austenitic steel surface. The characterisation should be completed, by using experimental methods well adapted to surface analysis.

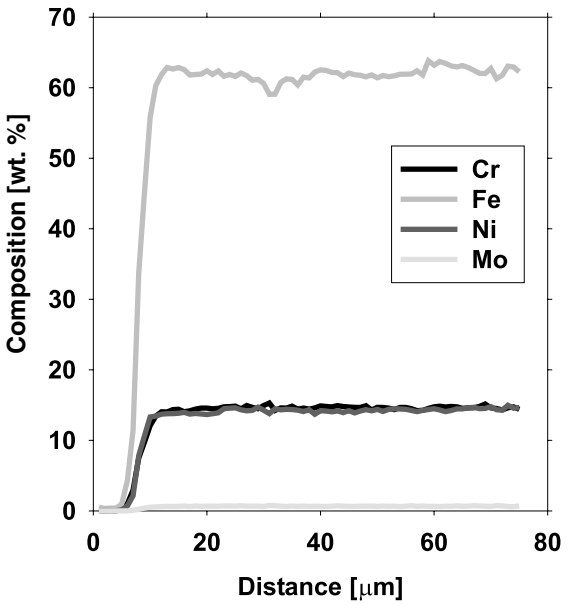

Fig. 8. Concentration profiles obtained on 1.4970 steel tested at 743 K for 3000 h.

4. Discussion

A good corrosion resistance was observed in all the steels tested at 573 K and up to 3000 h of exposure to liquid Pb–Bi.

At higher temperature (743 K), the austenitic steels (AISI 316L and 1.4970) did not exhibit dissolution of nickel in presence of Pb–Bi (which is currently observed with lead–lithium alloys [3]). In fact, a very thin (less than 1 µm) protective oxide layer was present on their surface. These steels, therefore, also have a good corrosion resistance in the testing conditions at 743 K.

At 743 K, the martensitic steels exhibited significant oxidation at their surfaces, with the oxide layers formed in the Pb–Bi–O liquid system preventing the dissolution of steels. For the Batman 27 and Batman 28 steels, the alloying elements such as Mn and W were present in the

observed corrosion products as described in the results. By analysing these corrosion products, it could be supposed that the outermost layer is composed of an Fe_3O_4–Mn_3O_4 solid solution. This supposition is supported by the observation reported in [5] where the same oxide is described on the surface of an Fe–4.9% Mn alloy. The composition detected in the inner layers could be connected to a spinel oxide of the type $(Fe, Cr)_3O_4$, as was observed in other works on martensitic steels conducted under stagnant conditions [6,7].

For the four martensitic steels (EM10, Optifer IVc, T91 and EP823), two layers were found in the oxidation zone. Regardless of the exposure time to Pb–Bi, the alloying elements were present mainly in the internal oxide layer with concentrations relative to their values in the metal slightly increased. In the case of the EP823 steel, silicon (about 3.5 wt%) was also was detected in the inner layer, this content being higher than in the substrate. The scale formed on these steels has the same morphology with porosity in the outer part. Analyses of the martensitic steels show that the outer layer consisted of magnetite Fe_3O_4 with the inner layer being a mixed spinel oxide $(Fe, Cr)_3O_4$. These results are in agreement with the high-temperature oxidation behaviour of Fe–9Cr steels [8] and with the behaviour of martensitic steels exposed to stagnant melts [6,7].

Concerning the oxidation kinetics of martensitic steels, the measured oxide layer thickness vs. time for each substrate is reported in Fig. 9. Assuming that the oxidation reaction is diffusion limited, the thickness data were interpolated by means of a parabolic law. It is shown that the Optifer IVc steel has the highest oxidation rate whereas the EP823 steel has the lowest. Therefore, the EP823 steel exhibits the best oxidation resistance at the test temperatures and the oxidation resistance of the different martensitic steels is classified as follows: EP823 > BA27 > T91 > BA28 > EM10 > Optifer IVc.

In order to clarify the different oxidation rates observed in the martensitic and austenitic steels tested under the same conditions, the effect of alloying elements has to be taken into account. In the literature there are no systematic studies on the effect of alloying elements on the oxidation rate of steels in the liquid metal system Pb–Bi–O, but it is possible to refer to general studies in the field of high-temperature oxidant environments. High-temperature oxidation studies performed on austenitic steels showed that a continuous oxide film grows on the surface [9,10]. In Fe–Cr binary alloys with relatively low Cr contents, a complex oxide scale forms on the surface with a corresponding increase in the oxidation rate of the steels [11–13]. In Pb–Bi, the higher oxidation resistance of the 1.4970 and the AISI 316L austenitic steels compared to that of the martensitic steels is thus well consistent, and the development of a protective oxide film on the surface of austenitic steels is very likely.

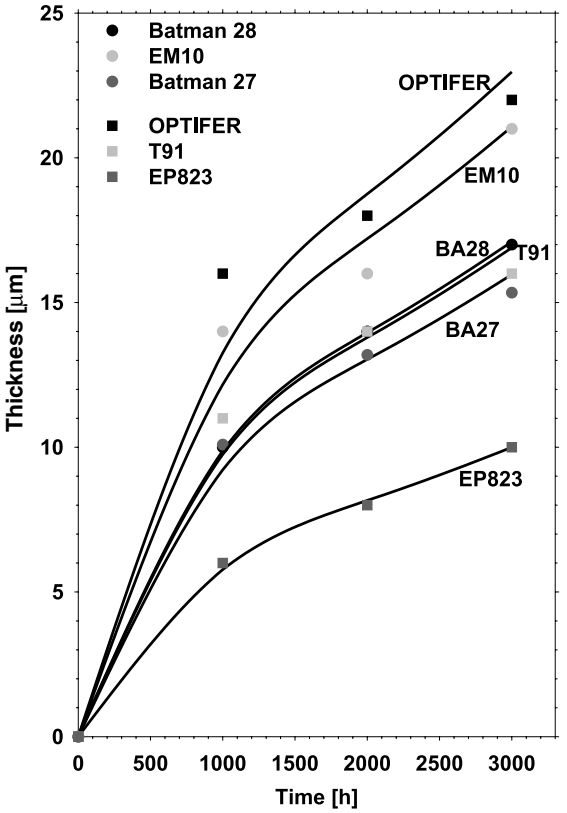

Fig. 9. Oxidation kinetics of the martensitic steels tested at 743 K. The measured oxide layer thicknesses are reported vs. the testing time and interpolated with a parabolic equation.

Referring to the martensitic steels tested at 743 K, the Fig. 9 shows that their oxidation behaviour depends on the substrate composition, which clearly indicates an influence of the alloying elements on the oxide growth process. Next, the effect of the various elements on oxidation is reported by comparing the effect with data on high-temperature oxidation reported in the literature cited below, taking care that the data do not refer specifically to Fe alloys containing the Cr contents presented in Table 1. Moreover, the temperature and the oxygen content were not the same and the elements may also interfere with each other, leading to a combination of effects. In the different steels herein tested, the Cr content varies from 8.3% to 12%. Only a slight effect of chromium on oxidation is expected in this range (Cr contents lesser than 8% are necessary to detect a clear change in the oxidation rate [13,14]) and the effect of the other alloying elements could be more significant. Silicon added to Fe–Cr alloys is known to reduce the growth rate of the oxide at 500°C [13,15]. Therefore, the good oxidation resistance obtained for EP823 steel

(which has the highest Si content – about 2%) is quite consistent. The effect of other metal additions such as Mn, Nb, V, W, Mo, Ti or Ni is more complex and, for some, there exists no general consensus. It is suggested that molybdenum has a neutral effect [16] or a deleterious effect so that an improvement in oxidation resistance of 9% chromium steels is obtained when the Mo content is reduced to a low level [15]. Mo is present in EM10 (1.0 wt%), T91 steel (0.95 wt%) and EP823 steel (0.7 wt%). By comparing the higher oxidation resistance of T91 with respect to EM10 steel (Fig. 9), it could be supposed that the other alloying elements in T91 (such as 0.20 wt% V, 0.075 wt% Nb, and 0.43 wt% Si) have a beneficial effect. In the same way, the Si content in EP823 steel (1.8 wt%) increases the oxidation resistance with respect to the EM10 steel. The influence of tungsten would be similar to that of molybdenum [13]. Referring to the kinetics in Fig. 9, it is evident that Optifer IVc and EP823 steels have an opposite behavior though W is present at the same concentration, but Si plays an important role in the EP823 steel. With regard to Batman 27 and Batman 28 steels, both have about 1.5 wt% of W and other alloying elements such as Si (0.3–0.4 wt%) and Mn (3.1–3.5 wt%) and an higher oxidation resistance. Moreover, by comparing the behaviour of the two Batman steels, it seems that 0.2 wt% of Ti (Batman 27) beneficially affects the oxidation resistance. From the results, Optifer IVc and EM10 steels without niobium addition are both less resistant to oxidation. It is thus suggested that the effect of Nb on the oxidation of steels could be beneficial. In the literature, the advantageous effect of Nb is reported in an Fe–17Cr alloy [14,16,17]. Although vanadium is present in the various steels (except the EM10), no significant effect of this element on the oxidation behavior could be detected in the frame of this study.

5. Conclusions

The present study led to the following conclusions.

(a) At 573 K, all the austenitic and martensitic steels exhibited good corrosion resistance. A very thin oxide film was formed on the surfaces, leading to protection against liquid metal corrosion.

(b) The results obtained at 743 K show that both categories of steels, austenitic and martensitic, produce stable protective oxide layers in the presence of Pb–Bi containing 10^{-6} wt% oxygen, which prevent the dissolution of steel elements in the Pb–Bi liquid alloy. The content of oxygen chosen for the tests was lower than the solubility of oxygen in Pb–55Bi at 572 K (about 2×10^{-5} wt% [18]) in order to avoid plugging of the loop. Despite being very thin (<1 μm), the layer is sufficient to protect the surface of austenitic steels against liquid metal corrosion, although it is much thicker for martensitic steels. With regard to protection, the thickness of the oxide layer must be limited to a purely beneficial value; otherwise failure and spalling of the scale could occur, leading to degradation of the steel.

(c) To summarise the influence of alloying elements on the oxidation rate of the martensitic steels, it can be suggested that tungsten and molybdenum have no effect or worse, a deleterious effect on the oxidation rate. Silicon is, for the most part, effective against oxidation of Fe–Cr martensitic steels exposed to liquid Pb–Bi, and a combination of niobium and titanium could be moderately beneficial.

Acknowledgements

The authors are grateful to N. Skvortzov, Y. Pevtchich and G. Yachmenev, IPPE, and F. Herbert, C. Blanc and C. Chénière, CEA, for their technical assistance in this work, to C. Martini, University of Bologna, for the recording and evaluation of the XRD spectra on the AISI 316L, EM10, Batman 27 and Batman 28 steels and to the ENEA-Brasimone Laboratory of Metallurgy for the specimen preparation assistance.

References

[1] C. Rubbia, J.A. Rubio, S. Buono, F. Carminati, Conceptual design of a fast neutron operated high power energy amplifier, CERN/AT/95-44 (ET), 1995.
[2] M. Broc, J. Sannier, G. Santarini, Behaviour of Ferritic Steels in the Presence of Flowing Purified Liquid Lead in Liquid Metal Engineering and Technology, BNES, London, 1984, p. 361.
[3] T. Flament, P. Tortorelli, V. Coen, H.U. Borgstedt, J. Nucl. Mater. 191–194 (1992) 132.
[4] F. Barbier, A. Rusanov, Corrosion behaviour of steels in flowing lead–bismuth, presented at the International Workshop on Spallation Materials Technology (IWSMT-4), Schruns, Austria, October 8–13, 2000, J. Nucl. Mater. 296 (2001) in press.
[5] O. Kubaschewski, B.E. Hopkins, Oxidation of Metals and Alloys, Butterworths, London, 1962.
[6] G. Benamati, P. Buttol, V. Imbeni, C. Martini, G. Palombarini, J. Nucl. Mater. 279 (2000) 308.
[7] G. Müller, G. Schumacher, F. Zimmermann, J. Nucl. Mater. 278 (2000) 85.
[8] P.C. Rowlands, D.R. Holmes, A. Whittaker, R.A. Brierley, J.C.P. Garrett, The Oxidation Behavior of Fe–9Cr–1Mo Steels in Gas-Cooled Reactors Today, BNES, London, 1983, p. 173.
[9] S. Shibagaki, A. Koga, Y. Shirakawa, H. Onishi, H. Yokokawa, J. Tanaka, Thin Solid Films 303 (1997) 101.
[10] F.S. Shieu, M.J. Deng, S.H. Lin, Corros. Sci. 40 (1998) 1267.
[11] N. Birks, G.H. Meir, Introduction to High Temperature Oxidation of Metals, Arnold, London, 1983.

[12] G.Y. Lai, High Temperature Corrosion of Engineering Alloys, ASM International, Materials Park, OH, 1990.
[13] J. Bénard (Ed.), Oxydation des Métaux, Gauthier-Villars, Paris, 1962.
[14] F. Armanet, J.H. Davidson, Les aciers inoxydables, in: L. Lacombe, B. Baroux, G. Beranger (Eds.), Les Editions de Physique, 1990, p. 448.
[15] R.A. Brierley, Studies of the Oxidation of 9 and 12 Cr Steels in High Temperature and High Pressure CO_2 in Corrosion of Steels in CO_2, BNES, London, 1974, p. 165.
[16] A. Ikeda, M. Ueda, S. Mukai, CO_2 Behavior of Carbon and Cr Steels in Advances in CO_2 Corrosion, in: R.H. Hausler, H.P. Godard (Eds.), National Association of Corrosion Engineers, Houston, TX, 1984, p. 39.
[17] T. Moroishi, H. Fujikawa, H. Makiura, J. Electrochem. Soc. 126 (1979) 2173.
[18] Yu.I. Orlov, B.F. Gromov, V.A. Gylevsky, in: Seminar on the Concept of Lead Cooled Fast Reactors, CEA, Cadarache, France, September 22–23, 1997 (quoted in ENEA Report VT-SBA-00001, 1997, p. 134).